

# Removal of Cr(VI) from aqueous solutions by using activated carbon supported iron catalysts as efficient adsorbents

Karima Derdour, Chafia Bouchelta, Amina Khorief Naser-Eddine and Mohamed Salah Medjram  
Laboratory LGCES, Faculty of Technology, 20 Août 1955 University of Skikda, Skikda, Algeria, and

Pierre Magri

Laboratory LCP-A2MC, University of Lorraine, Metz, France

## Abstract

**Purpose** – The purpose of this paper is to focus on the removal of hexavalent chromium [Cr(VI)] from wastewater by using activated carbon-supported Fe catalysts derived from walnut shell prepared using a wetness impregnation process. The different conditions of preparation such as impregnation rate and calcination conditions (temperature and time) were optimized to determine their effects on the catalyst's characteristics.

**Design/methodology/approach** – The catalyst samples were characterized using thermogravimetric analysis, scanning electron microscopy and Fourier transform infrared spectroscopy. The adsorption of Cr(VI) by using activated carbon supported Fe catalysts derived from walnut shell as an adsorbent and catalyst was investigated under different adsorption conditions. The parameters studied were contact time, adsorbent dose, solution pH and initial concentrations.

**Findings** – Results showed that higher adsorption capacity and rapid kinetics were obtained when the activated walnut shell was impregnated with Fe at 5 per cent and calcined under N<sub>2</sub> flow at 400°C for 2 h. The adsorption isotherms data were analyzed with Langmuir and Freundlich models. The better fit is obtained with the Langmuir model with a maximum adsorption capacity of 29.67 mg/g for Cr(VI) on Fe5-AWS at pH 2.0.

**Originality/value** – A comparison of two kinetic models shows that the adsorption isotherms system is better described by the pseudo-first-order kinetic model.

**Keywords** Adsorption, Activated carbon, Hexavalent chromium, Iron catalysts, Walnut shell, Wetness impregnation

**Paper type** Research paper

## 1. Introduction

Pollution endangers the environment, and heavy metal pollution is one of the most hazardous type of pollution when detected beyond certain amounts. Heavy metals affect plants, humans and the latter can suffer from a lot of diseases such as cancer, allergies and even birth defects (Jianping *et al.*, 2009). One of the most toxic and harmful heavy metals is Cr. It is usually present in textile industries, paint, paper, leather tanning and petroleum refining processes, in addition to industrial effluents such as electroplating (Ahmad *et al.*, 2011). The two natural states of Cr are the trivalent Cr(III) and hexavalent Cr(VI). Cr(VI) is 500 times more toxic than Cr(III) because of its properties such as its rapid mobility and instant solubility in aqueous solutions. The US Environmental Protection Agency has set the maximum permissible level of Cr(VI) discharge in wastewater at 0.05 mg·L<sup>-1</sup> (Parinda and Paitip, 2012; Yuanyuan *et al.*, 2014).

To remove or to minimize the presence of Cr(VI) from wastewater, different methods can be adopted, such as chemical precipitation (Thomson and Miller, 1998), ion

exchange (Cavaco *et al.*, 2009), oxidation/reduction (Daulton *et al.*, 2007; Olmez, 2009), membrane processes (Melita and Popescu, 2008) and the adsorption on activated carbon (Liu *et al.*, 2010). Compared to other methods, adsorption on activated carbon has been proved to be a sufficient and effective method because of it is easily operation and economic advantages and metal ions can be completely removed even at low concentrations (Uysal and Ar, 2007; Xiang *et al.*, 2017). As a consequence, the necessity of finding more effective adsorbents became apparent, but at the same time, it should be at a lower cost (Dubey and Gopal, 2007). The availability of agricultural wastes made them susceptible to be used as cheap adsorbents because they are considered unused resources and environment-friendly (Wei *et al.*, 2013). Agricultural waste products such as almond shell (Agarwal *et al.*, 2006), apricot stone (Erhan *et al.*, 2004), coir pith (Thomson and Miller, 1998), orange peel (Park *et al.*, 2007), rice husk (Sumathi *et al.*, 2005), grape waste (Chand *et al.*, 2009) and waste tea (Orhan and Buyukgungor, 1993) can recently be the source of adsorbents to remove Cr(VI) from wastewater. The use of carbon as an adsorbent is not as effective in removing organic compounds as in eliminating metals and inorganic pollutants. To enhance the aforementioned products' adsorption capacity, their characteristics would be modified with certain chemicals (Wang *et al.*, 2011; Pehlivan *et al.*, 2013).

The current issue and full text archive of this journal is available on Emerald Insight at: [www.emeraldinsight.com/1708-5284.htm](http://www.emeraldinsight.com/1708-5284.htm)



World Journal of Engineering  
15/1 (2018) 3–13  
© Emerald Publishing Limited [ISSN 1708-5284]  
[DOI 10.1108/WJE-06-2017-0132]

Received 9 June 2017  
Accepted 26 July 2017

The widespread use of impregnated activated carbon as a catalyst and, at the same time, adsorbent is attributed to its high surface area and other characteristics such as the porous structure, surface functional groups and, above all, chemical stability (Irfan *et al.*, 2015; Asma *et al.*, 2015). Late findings have proven that the capacity of activated carbon to adsorb Cr(VI) is notably higher when it is impregnated with metal oxides such as Fe (hydr) oxides (Phuengprasop *et al.*, 2011). The mechanisms of the elimination of hexavalent chromium [Cr(VI)] are explained by electrostatic attraction, ion exchange and surface complexation.

The main purpose of this study is:

- to prepare activated carbon from walnut shell by physical activation; and
- to use it as a supporting material for Fe oxides to enhance adsorption capacity and the adsorption kinetics of Cr(VI).

Some factors have been taken into consideration for the preparation of the final catalyst, such as the impregnation rate and the calcination conditions (temperature and time), to observe their effect on the properties of the result catalyst, mainly its catalytic activity and adsorption capacity.

## 2. Materials and methods

### 2.1 Preparation of synthetic solution

All used chemicals and reagents were of analytical grade. A stock solution of  $1,000 \text{ mg}\cdot\text{L}^{-1}$  of Cr(VI) was prepared by dissolving 2.8289 g of  $\text{K}_2\text{Cr}_2\text{O}_7$  salt in 1,000 mL of distilled water. The desired solutions with different concentration of Cr(VI) were prepared by dilution of the stock solution. The Cr(VI) concentration was measured by reacting Cr(VI) with 1,5-diphenylcarbazide, which forms a red-violet-colored complex and determining the absorbance of the solution with a spectrophotometer (1800 SHIMADZU) at  $\lambda_{\text{max}} = 540 \text{ nm}$ .

The initial pH of the test solutions was adjusted to the desired value by using dilute solutions of HCl and NaOH.

### 2.2 Starting material

Walnut shells were locally collected. First, they were cleaned with distilled water and dried at  $105^\circ\text{C}$  for 24 h to remove water and then mixed with  $\text{H}_2\text{SO}_4$  solution prepared at 40 per cent under constant shaking for 4 h at ambient temperature. The produced solid was then washed with distilled water until the pH of the filtrating solution became neutral. Finally, the cleaned samples were dried in an oven at  $110^\circ\text{C}$  till constant weight was obtained. The dried sample was crushed and sieved into particles sized less than 0.5 mm in diameter.

### 2.3 Activation procedure

Activated carbons were prepared from walnut shells by pyrolysis and physical activation under water vapor/ $\text{N}_2$  for 2 h at  $10^\circ\text{C}\cdot\text{min}^{-1}$  in a tubular electrical furnace (Chafia *et al.*, 2012). Different pyrolysis temperatures (700, 800, 900 and  $1,000^\circ\text{C}$ ) were used to study the effect of temperature on the char structures.

### 2.4 Catalyst preparation

Activated carbon-supported Fe catalysts were prepared using an incipient wetness impregnation utilizing aqueous Fe(III) nitrate nonahydrate [ $\text{Fe}(\text{NO}_3)_3\cdot 9\text{H}_2\text{O}$ , 98.6 per cent from

Sigma-Aldrich]. In brief, 2 g of AWS 900 was mixed with  $\text{Fe}(\text{NO}_3)_3\cdot 9\text{H}_2\text{O}$  in 40 mL of a mixture of distilled water and ethanol (75 per cent distilled water and 25 per cent ethanol) to obtain final catalysts with Fe content equal to 5, 10 and 15 per cent. After that, NaOH was added to achieve a final pH of 11 to permit the precipitation of Fe species on the surface of the activated walnut shell as Fe oxides. The mixture was stirred under constant shaking for 24 h at ambient temperature and then ultrasonicated for 2 h to obtain complete penetration and saturation of the metal ions in the activated carbon pores (Wei *et al.*, 2013). After the solvent was evaporated and the catalyst precursor was washed several times with distilled water until a neutral pH was obtained, it was then dried in an oven at  $110^\circ\text{C}$  for about 24 h. Finally, the obtained material was calcined under  $\text{N}_2$  flow at different temperatures (300, 400 and  $500^\circ\text{C}$ ) for three calcinations durations (1, 2 and 3 h). The step of calcination is carried out to remove counter-Fe of the metallic cation and, as a result, to fix the metallic groups on the carbon matrix (Hero *et al.*, 2012). The nomenclature used to denote the walnut shell samples treated under different conditions are given in Table I.

## 3. Characterization of the adsorbents

Thermogravimetric analysis (TGA/derivative thermogravimetric [DTG]) allows continuous recording of sample mass changes with linearly increasing temperature. The used apparatus was a 2050 TGA V4.5A from TA Instruments. The thermal evolution of raw materials and

Table I Nomenclature used for the preparation of Fe-activated carbon catalysts under different conditions

Sample treatment	Nomenclature
Raw walnut shells	RWS
Activated walnut shells at 700, 800, 900 and $1,000^\circ\text{C}$ (for 2 h, $150 \text{ cm}^3\cdot\text{min}^{-1}$ $\text{N}_2$ flow rate and $10^\circ\text{C}\cdot\text{min}^{-1}$ heating rate)	AWS 700, AWS 800, AWS 900, AWS 1000
Activated walnut shells impregnated with 5% of Fe and calcined at $400^\circ\text{C}$ for 2 h	Fe5-AWS
Activated walnut shells impregnated with 10% of Fe and calcined at $400^\circ\text{C}$ for 2 h	Fe10-AWS
Activated walnut shells impregnated with 15% of Fe and calcined at $400^\circ\text{C}$ for 2 h	Fe15-AWS
Activated walnut shells impregnated with 5% of Fe and calcined at $300^\circ\text{C}$ for 2 h	Fe5-AWS/300
Activated walnut shells impregnated with 5% of Fe and calcined at $500^\circ\text{C}$ for 2 h	Fe5-AWS/500
Activated walnut shells impregnated with 5% of Fe and calcined at $400^\circ\text{C}$ for 1 h	Fe5-AWS/1
Activated walnut shells impregnated with 5% of Fe and calcined at $400^\circ\text{C}$ for 3 h	Fe 5-AWS/3

activated carbons was measured using TGA from room temperature up to 900°C. The average mass of the analyzed samples was about 8.60 mg and 22 mg for raw material and activated carbon, respectively.

The morphologies of activated carbon produced from walnut shells and Fe-impregnated activated carbons were observed using scanning electron microscopy (SEM) (High Resolution Quanta FEI 200).

Identification of surface functional groups of the raw walnut waste, the resulting activated carbon and impregnated activated carbons was carried out by using Fourier transform infrared (FTIR) spectroscopy. The infrared transmission spectra were obtained using a spectrometer of Perkin Elmer (Spectrum One FTIR) in the scanning range of 4,000-650  $\text{cm}^{-1}$  and using the KBr wafer technique.

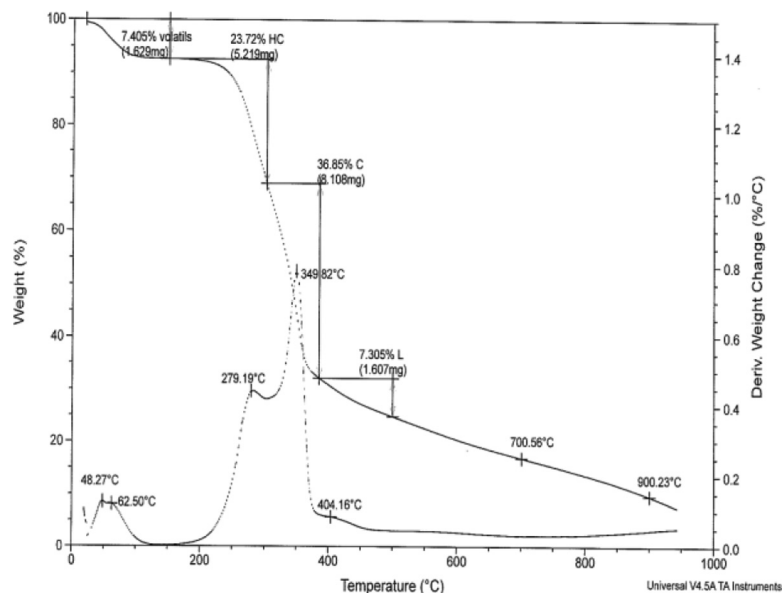
## 4. Batch sorption studies

### 4.1 The effect of contact time

In every transfer phenomenon, contact time is undoubtedly a crucial parameter. In adsorption, the equilibrium time indicates the possible diffusion control mechanism between the adsorbate as it moves toward the adsorption surface (Yuanyuan *et al.*, 2014). Here, 1 g of each adsorbent was thoroughly mixed with 100 mL Cr(VI) solution in a 200 mL glass flask under initial Cr(VI) concentration of 100  $\text{mg}\cdot\text{L}^{-1}$ . Adsorption kinetics of Cr(VI) were studied at room temperature of 25°C and at pH 2. At certain time intervals, 1 mL of the solution mixture was extracted and the residual concentrations of Cr(VI) were measured using an ultraviolet-visible (UV-vis) spectrophotometer. The amount of Cr(VI) per unit weight of adsorbent at time  $t$ ,  $q_t$ , was calculated using the following equation (1):

$$q_t = \frac{(C_0 - C_t) \times V}{m} \quad (1)$$

Figure 1 TGA/DTG analysis of RWS



where  $C_0$  is the initial Cr(VI) concentration and  $C_t$  is the Cr(VI) concentration ( $\text{mg}\cdot\text{L}^{-1}$ ) at any time  $t$ ,  $V$  is the volume of the solutions (L) and  $m$  is the mass of the used adsorbents (g).

### 4.2 Effect of adsorbent dosage on Cr(VI) adsorption

The influence of the Fe5-AWS dose on the equilibrium uptake of Cr(VI) ions was studied in a batch reactor at room temperature of 25°C by varying the adsorbent from 0.2 to 1 g with an initial Cr(VI) concentration of 10  $\text{mg}\cdot\text{L}^{-1}$  at pH 2 and an initial volume of 100 mL for the corresponding contact time.

### 4.3 Effect of pH on metal adsorption

To evaluate the effect of initial solution pH on Fe5-AWS adsorption capacity, 0.6 g of this material was mixed with 100 mL of known Cr(VI) solution concentration of 10  $\text{mg}\cdot\text{L}^{-1}$  at different initial pH values of 2, 4, 6, 8 and 10 at room temperature of 25°C by using 200 rpm agitation speed for the contact time. pH was adjusted using 0.1M HCl or 0.1M NaOH.

### 4.4 Sorption isotherms

Adsorption isotherm experiments were carried out in a 200 mL glass flask, at a constant temperature of 25°C, containing 0.6 g of Fe5-AWS and 100 mL of Cr(VI) solutions with various initial concentrations (10, 30, 60, 120, 200, 300 and 400  $\text{mg}\cdot\text{L}^{-1}$ ) with the predetermined optimum pH values and agitated at 200 rpm for obtaining the equilibrium time. The concentrations of Cr(VI) were measured using UV-vis spectrophotometer at  $\lambda_{max} = 540 \text{ nm}$ . The adsorption capacity at equilibrium ( $q_e$ ) was calculated using the following equation:

$$q_e = \frac{(C_0 - C_e) \times V}{m} \quad (2)$$

where  $C_0$  and  $C_e$  are the initial and the equilibrium concentrations of Cr(VI) in the solution ( $\text{mg}\cdot\text{L}^{-1}$ ), respectively,  $V$  is the total volume of solution (L) and  $m$  is the adsorbent dosage (g).

Two adsorption models (Langmuir and Freundlich) were applied to the experimental data (Chafia *et al.*, 2012). The linear expression for the Langmuir isotherm is represented as:

$$\frac{C_e}{q_e} = \frac{C_e}{q_m} + \frac{1}{K_L q_m} \quad (3)$$

where  $C_e$  is the equilibrium concentration of ions ( $\text{mg}\cdot\text{L}^{-1}$ ),  $q_e$  is the amount of the metallic ions adsorbed ( $\text{mg}\cdot\text{g}^{-1}$ ),  $q_m$  is the maximal adsorption capacity ( $\text{mg}\cdot\text{g}^{-1}$ ) and  $K_L$  is the Langmuir equilibrium constant ( $\text{L}\cdot\text{g}^{-1}$ ).

The Freundlich model is given by the linear equation:

$$\log q_e = \log K_F + \frac{1}{n} \log C_e \quad (4)$$

where  $q_e$  is the amount adsorbed ( $\text{mg}\cdot\text{g}^{-1}$ ),  $C_e$  is the equilibrium concentration of the adsorbate ( $\text{mg}\cdot\text{L}^{-1}$ ) and  $K_F$  and  $n$ , the Freundlich constants, are related to adsorption capacity and adsorption intensity, respectively.

## 5. Results and discussion

### 5.1 Properties of RWS, AWS 900 and Fe-AWS

#### 5.1.1 Thermogravimetric analyses

TGA and DTG curves of the raw walnut shell are shown in Figure 1. TGA profile shows that the process of weight loss contained four sections. First, the weight loss of 7.405 per cent at  $48.27^\circ\text{C}$  could be due to water evaporation. At the second stage, the process of decomposition attains 23.72 per cent weight loss at the maximum rate of  $279.2^\circ\text{C}$ . In the third stage, mass loss of 36.85 per cent is observed at  $349.82^\circ\text{C}$ . The last mass loss was 7.303 per cent, and it occurred at the temperature of  $404.16^\circ\text{C}$ . Previous findings in accordance with our results show that walnut shell loses its weight between  $250$  and  $380^\circ\text{C}$ . However, cellulose degrades thermally between  $315$  and  $400^\circ\text{C}$ , and lignin is more thermostable than both cellulose and hemicellulose, and its range of decomposition is very wide (Su-Hwa *et al.*, 2014).

Figure 2 TGA/DTG analysis of AWS

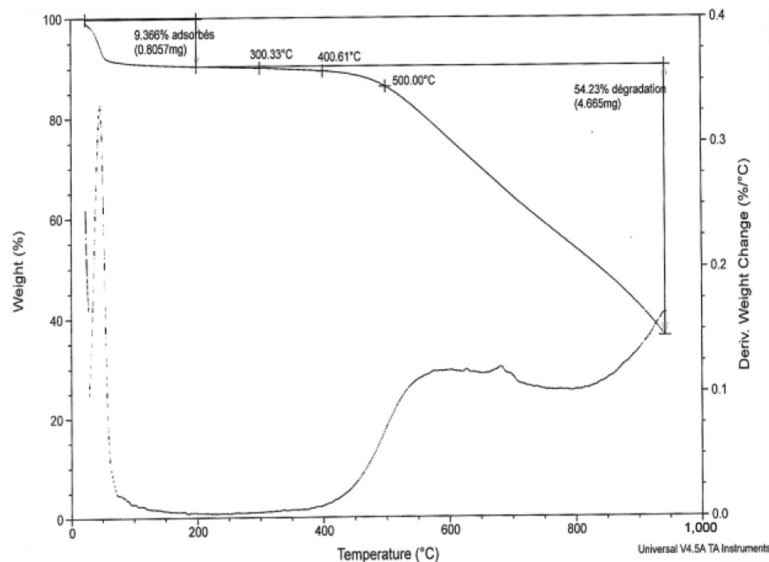
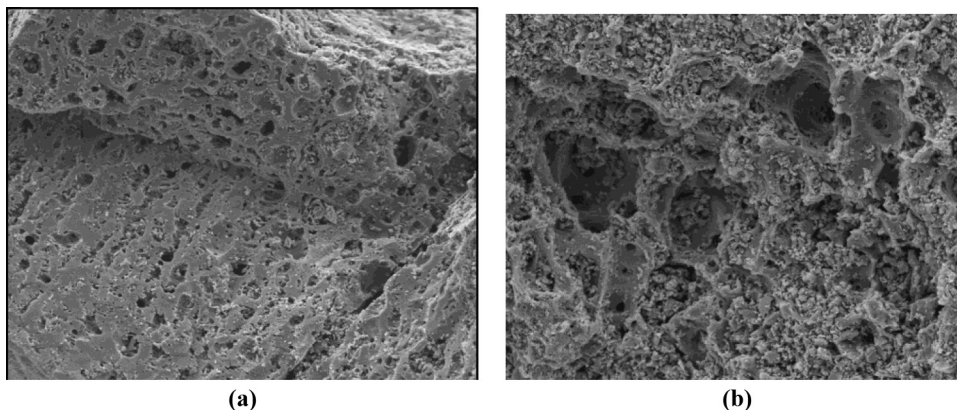


Figure 3 Scanning electron micrographs of a) AWS 900 and b) Fe5-AWS samples



The (TGA/DTG) thermal curve corresponding to activated walnut shell is shown in Figure 2. From this figure, we can see little degradation in the range of 300-400°C, but starting from 500°C, an important mass loss (54.23 per cent) was observed, which can be attributed to the remaining lignin decomposition.

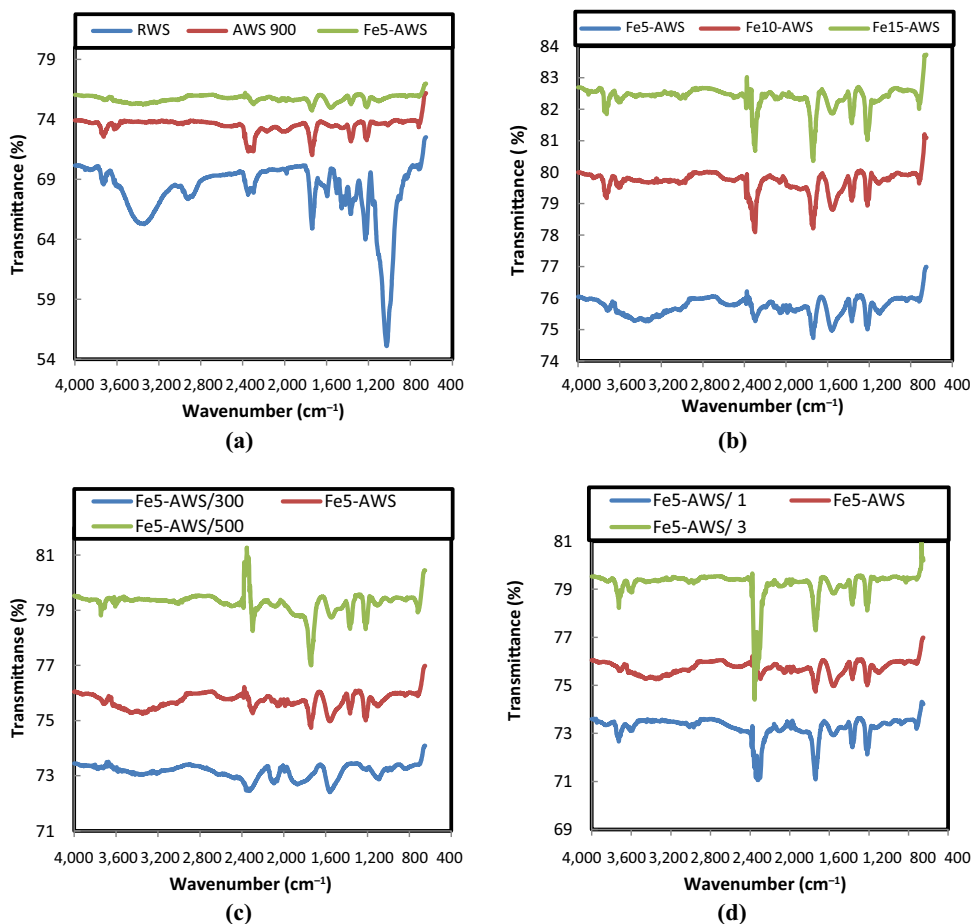
### 5.1.2 Scanning electron microscopy

The surface morphology of the prepared materials observed using SEM is shown in Figure 3. SEM images showed that pores with different sizes and different shapes existed on the external surface of AWS and Fe-AWS. It is observed that the virgin activated carbon [Figure 3(a)] was relatively smooth and flat. After modification, the surface of the Fe-AWC was much rather rough [Figure 3(b)], proving that the metal ions were successfully loaded on the activated carbon.

### 5.1.3 Fourier transform infrared spectra analysis

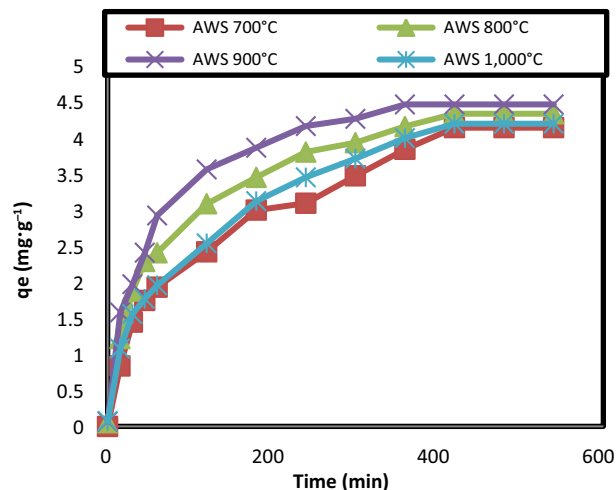
The FTIR spectra of RWS, AWS and Fe-AWS are illustrated in Figure 4. The peaks at 3,740 and 3,400  $\text{cm}^{-1}$  are assigned to  $-\text{NH}_2$  stretching (Ghadir et al., 2015) and  $-\text{OH}$  stretching of hydroxyl groups (Mohammed et al., 2012). The bands located at 2,921 and 2,348  $\text{cm}^{-1}$  are attributed to C-H asymmetric stretching vibration in methyl and  $\text{C}\equiv\text{C}$  group, respectively (Ghadir et al., 2015; Jia-Shun et al., 2014; Yahia and Hisham, 2009; Maryam et al., 2008).

**Figure 4** FTIR spectra of a) RWS, AWS 900, Fe5-AWS, b) Fe5-AWS, Fe10-AWS, Fe15-AWS, c) Fe5-AWS/300, Fe5-AWS, Fe5-AWS/500 and d) Fe5-AWS/1, Fe5-AWS, and Fe5-AWS/3



Carbonyl groups  $\text{C}=\text{O}$  appeared at 1,740  $\text{cm}^{-1}$  and  $\text{C}=\text{C}$  ring stretch of aromatic rings appeared at 1,600  $\text{cm}^{-1}$  (Xiang et al., 2017; Muhammad et al., 2014). The bands at around 1,455 and 1,376  $\text{cm}^{-1}$  corresponded to the C-H

**Figure 5** Effect of pyrolysis temperatures of AWS on the adsorption of Cr(VI) ( $T = 25^\circ\text{C}$ ,  $\text{pH} = 2$ , dosage = 1 g/100 mL and  $C_0 = 45 \text{ mg}\cdot\text{L}^{-1}$ )



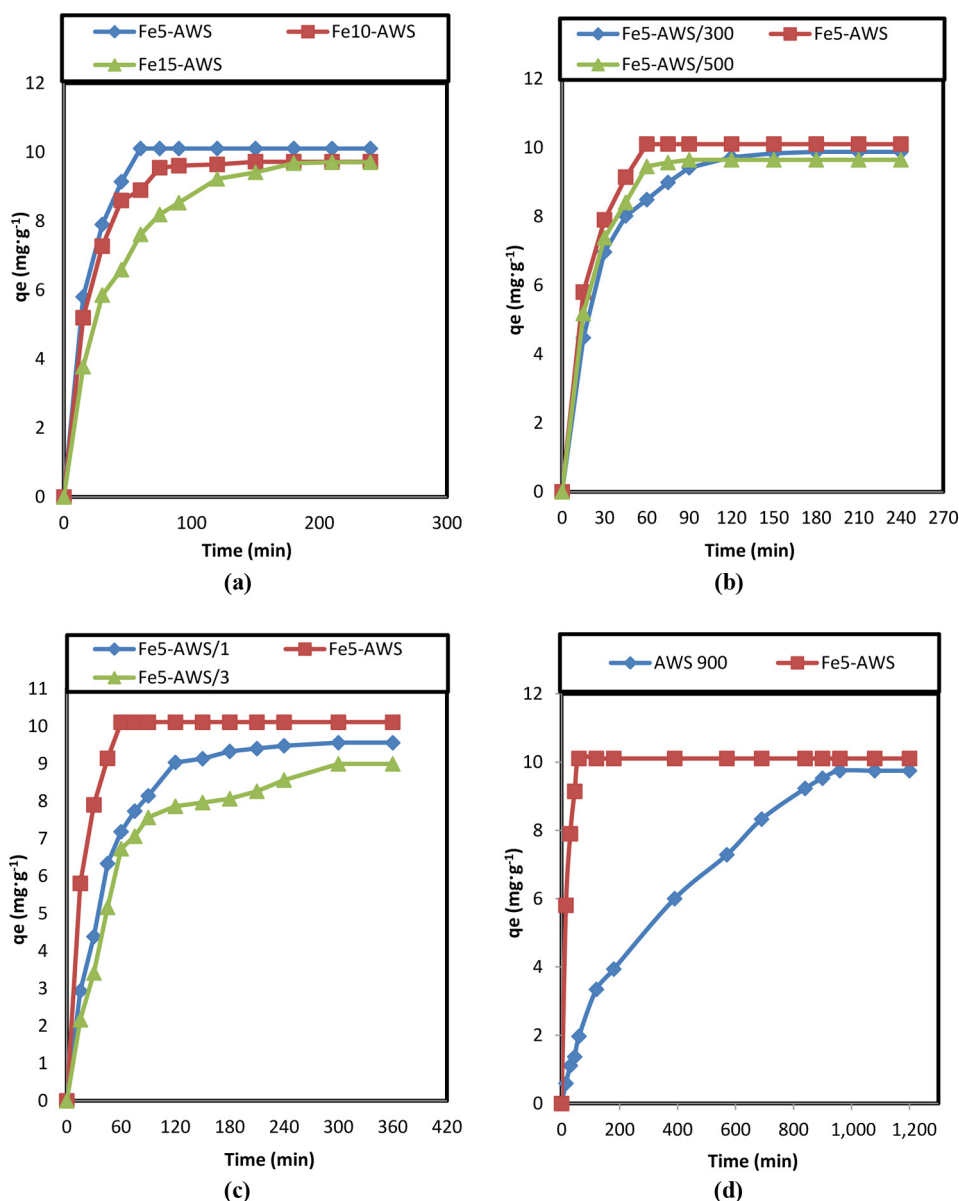
in-plane bending vibrations in methyl and methylene groups, and bands at  $1,235$  and  $1,033\text{ cm}^{-1}$  are attributed to C-O stretching vibration in alcohols, phenols or ether groups (Jia-Shun *et al.*, 2014; Juan and Keqiang, 2010). Finally, the band at  $720\text{ cm}^{-1}$  is attributed to C-H deformation in cellulose (Asmaa and Muthanna, 2016). After activation, the peaks corresponding to the O-H groups and aliphatic groups became weaker or disappeared. A strong peak attributed to  $\text{C}\equiv\text{C}$  groups is observed at  $2,000\text{ cm}^{-1}$  because of the increase in aromaticity of RWS after activation at high temperature. FTIR spectrum of Fe-AWS show the same bands observed in AWS; however, a new strong band appeared at  $1,558\text{ cm}^{-1}$  and a weak band appeared at  $2,296\text{ cm}^{-1}$ , which are ascribed to carboxylates existing on Fe-AWS (Jian-hong *et al.*, 2015).

## 5.2 Adsorption experiments

### 5.2.1 Effect of pyrolysis temperature

The effect of pyrolysis temperature for AWS on adsorption of Cr(VI) is shown in Figure 5. It was shown that the Cr(VI) removal increased with increasing temperature up to  $900^\circ\text{C}$ , and then decreased at higher temperature. In the adsorption experiments applied on AWS pyrolyzed at  $700$ ,  $800$ ,  $900$  and  $1,000^\circ\text{C}$ , the Cr(VI) removal was  $91.97$ ,  $96.22$ ,  $99.11$  and  $93.17$  per cent, respectively. This is due to the elimination of volatile matters and the decomposition of important compounds such as cellulose and hemicellulose in the walnut shell which forms basic pores in the materials at the higher pyrolysis temperature. Therefore, the optimal pyrolysis temperature is then fixed at  $900^\circ\text{C}$ , and the results are confirmed by the results obtained using ATG analysis.

**Figure 6** a) Effect of the impregnation rate, b) effect of the calcination temperature and c) effect of the calcination time on the contact time and on the adsorption capacity of Cr(VI) and d) adsorption kinetics of Cr(VI) on Fe5-AWS and AWS 900



### 5.2.2 Effect of contact time

The contact time of the samples prepared was impacted by the initial Fe content, temperature and calcination time of precursors. Figure 6(a) shows the effect of the impregnation rate on the adsorption capacity from Cr(VI) and the contact time evolution. It can be seen that the removal of Cr(VI) is extremely faster in the first 30 min and tends to become slow with agitation time. Then, the system reached equilibrium after 60, 75 and 120 min for Fe5-AWS, Fe10-AWS and Fe15-AWS, respectively. It also can be found that the adsorption capacity decreased with increasing impregnated Fe content in the order Fe5-AWS > Fe10-AWS > Fe15-AWS. These results suggest that at a higher concentration (15 per cent), Fe particles plugged the carbon pores, thus lowering the surface area; therefore, the adsorption kinetic was a little slow and the adsorption capacity was low. The relation between the calcination temperature and the removal of Cr(VI) is described in Figure 6(b), and the maximum adsorption capacity is observed at 400°C, which is mainly due to the development of the porosity of the catalyst at this temperature. For the calcination time, it can be seen from Figure 6(c) that adsorption capacity increases when the heating time increases from 1 to 2 h, whereas when the heating time increases to 3 h, the adsorption capacity decreases, and the adsorption equilibrium on Fe5-AWS/1, Fe5-AWS and Fe5-AWS/3 is reached after 120, 60 and 300 min, respectively. This can be explained by the destruction of the structure of the catalyst at high heating temperatures. Consequently, we consider that optimal conditions are obtained when the activated walnut shell was impregnated with Fe at 5 per cent and calcined under N<sub>2</sub> flow at 400°C for 2 h.

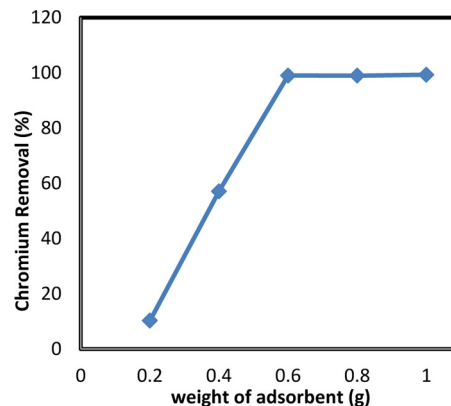
The kinetic curves obtained for Cr(VI) removal from aqueous solutions onto AWS 900 and Fe5-AWS are shown in Figure 6(d). It can be observed that activated carbon-supported Fe enhances the adsorption kinetics, and it is worth noting that about 99.63 per cent Cr(VI) was removed in 60 min, and on the other hand, at the same time, only 19.46 per cent of Cr(VI) was removed on AWS 900. The adsorption equilibrium is reached after 60 and 840 min of contact time for Fe5-AWS and AWS 900, respectively. It appears also that impregnated activated carbon has a small amelioration on the adsorption capacity of Cr(VI) compared to activated carbon used without modification.

Looking at the findings, we can understand the effect of Fe insertion on the surface of activated carbon. Fe oxides, mainly amorphous forms have a high affinity and selectivity for Cr(VI) oxyanions. Impregnating Fe (hydr) oxides into activated carbon can be positively seen on both levels of high selectivity of ferric oxides for Cr(VI) and the high surface area of activated carbon that offers adequate reactive sites for Fe loading (Liu et al., 2010).

### 5.2.3 Effect of adsorbent dosage

The effect of the amount of Fe5-AWS on biosorption of Cr(VI) was investigated by varying the biosorbent mass from 0.2 to 1 g for optimum contact time. The results obtained from Figure 7 show that the Cr(VI) removal increased with an increase in adsorbent amount and reaches saturation at about 0.6 g·L<sup>-1</sup>; this is due to reduction of greater number of active adsorption sites, so 0.6 g·L<sup>-1</sup> was chosen as the optimum adsorbent dose for further experiments.

**Figure 7** Effect of adsorbent dose on the adsorption of Cr(VI) by Fe5-AWS



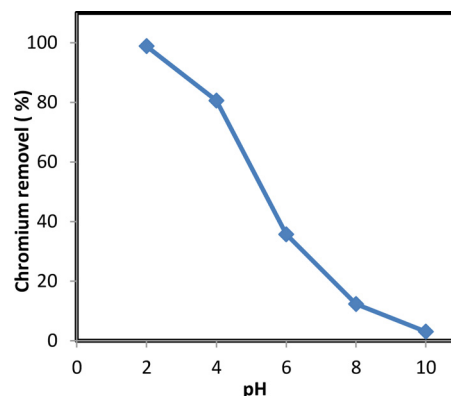
### 5.2.4 Effect of pH

The pH of the solution represents an important parameter in the adsorption of heavy metals at the surface of the adsorbent, because of the affects such as the solubility of adsorbate, concentration of the counter ions on the functional groups of the adsorbent and the degree of ionization of the adsorbate during reaction (AL-Othman et al., 2012). The effect of pH on the adsorption of Cr(VI) onto the surface of Fe5-AWS is presented in the Figure 8, which shows that the pH value increased from 2 to 10 and the removal efficiency decreased significantly from 98.89 to 3.1 per cent. Optimum pH was 2, and all other experiments were done at this pH. In an acid medium, the surface of the adsorbent is highly protonated and thus consequently favors the adsorption of Cr(VI) in its predominant anionic form of  $\text{HCrO}_4^-$ . Hence, sorption increases with an increase in the acidity of the solution. As the pH of the aqueous phase is increased, the adsorption of Cr(VI) ions decreases. This can be explained by the dissociation of the active sites on the surface of the adsorbent, which become negatively charged, thus causing the repulsion of the negatively charged metals.

### 5.2.5 Adsorption isotherms

Adsorption isotherm indicates the retention mechanism of the solution components to a solid-phase at equilibrium.

**Figure 8** Effect of pH on the adsorption of Cr(VI) on Fe5-AWS



Adsorption equilibrium is established when the ratio between the adsorbed amount with that remaining in the solution becomes constant (Nabil *et al.*, 2015). Adsorption isotherm of Cr(VI) on Fe5-AWS is reported in Figure 9(a). The isotherm was of Type I. Results indicate a high affinity and mean that at low concentrations of Cr(VI), the adsorption is total. The maximal Cr(VI) adsorption capacity determined at the plateau of the isotherm is  $29.673 \text{ mg}\cdot\text{g}^{-1}$ . The equilibrium adsorption data were interpreted using Langmuir and Freundlich models [Figure 9(b) and (c)]. The parameters of the isotherm models determined using regression analysis of the experimental data are given in Table II. The values of the correlation coefficient ( $R$ ) are higher for the Langmuir model than for the Freundlich model; this means that the Langmuir isotherm equation better represents the process of adsorption of Cr(VI) on activated carbon-supported Fe catalysts. This is probably due to the uniform distribution of active sites on the surface of the prepared catalyst. The  $n$  value in the Freundlich model was greater than 1 ( $n > 1$ ), indicating favorable adsorption of Cr(VI) on Fe5-AWS.

### 5.2.6 Adsorption kinetics

Knowledge of the adsorption kinetics in operations based on the adsorption phenomenon is of considerable practical interest for the optimal use of an adsorbent and for knowing the factors

**Table II** Langmuir and Freundlich parameters for Cr(VI) adsorption on Fe5-AWS

Langmuir isotherm model			Freundlich isotherm model		
$q_m \text{ (mg}\cdot\text{g}^{-1})$	$K_L \text{ (L}\cdot\text{mg}^{-1})$	$R$	$K_F \text{ (mg}\cdot\text{g}^{-1})$	$n$	$R$
29.673	0.093	0.983	9.963	5.214	0.960

that must be optimized to manufacture or improve an adsorbent to obtain fastest possible kinetics. To investigate the mechanism of adsorption, two kinetic models, namely, the pseudo-first-order and pseudo-second-order models, were applied (Samson and Adedibu, 2016). The linear form of Lagergren equation for pseudo-first-order adsorption kinetics is given by the following equation:

$$\ln(q_e - q_t) = \ln q_e - K_1 t \quad (5)$$

where  $q_e$  and  $q_t \text{ (mg}\cdot\text{g}^{-1})$  are the adsorption capacities at equilibrium time and time  $t$ , respectively,  $K_1 \text{ (L}\cdot\text{min}^{-1})$  is the pseudo-first-order rate constant. From plotting  $\log(q_e - q_t)$  versus  $t$  (Figure 10) and  $K_1$  and  $q_e$  can be obtained from the slope and intercept, respectively.

The equation of pseudo-second-order kinetic model is as follows:

**Figure 9** a) Modeling of adsorption isotherm of Cr(VI) on Fe5-AWS, b) linearized Langmuir model and c) linearized Freundlich model

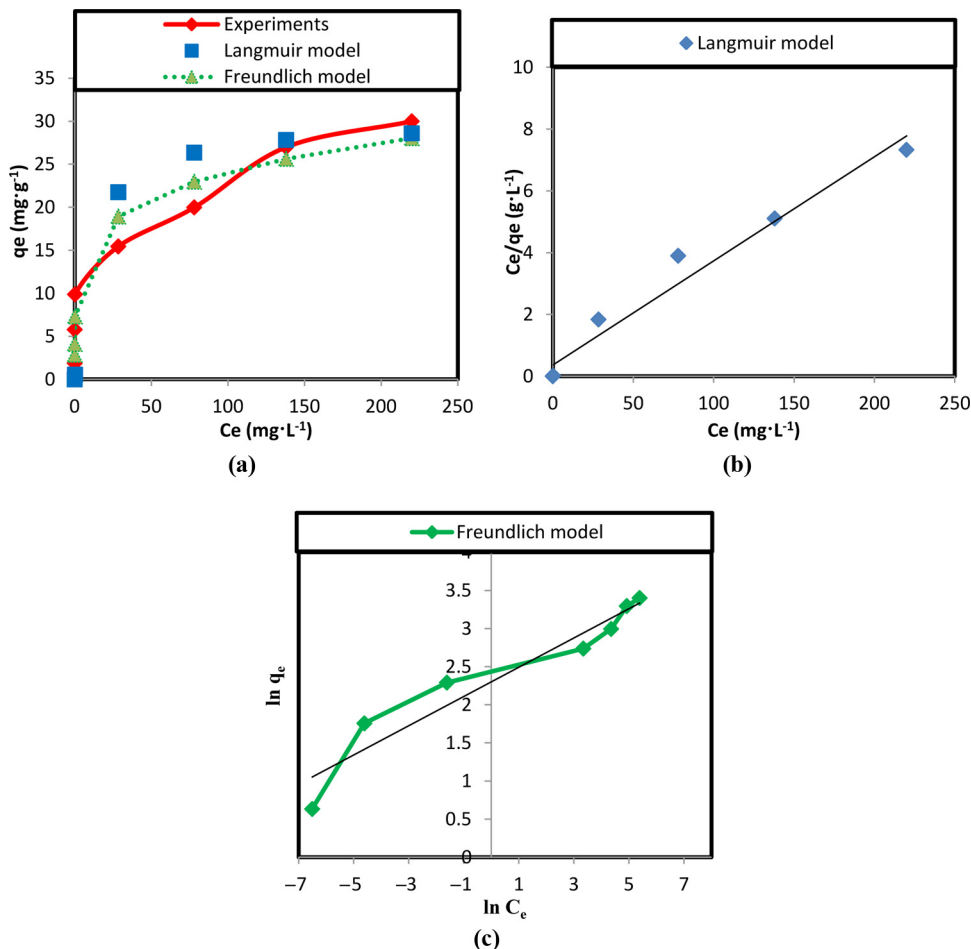
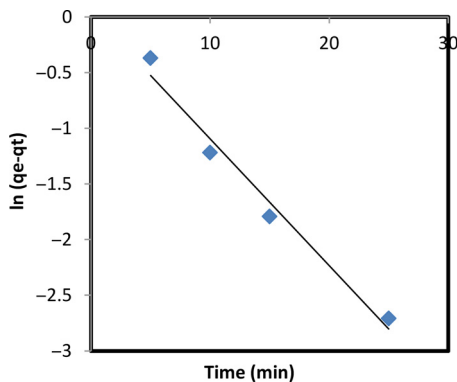


**Figure 10** Pseudo-first-order kinetic plot for the adsorption of Cr(VI) removal from aqueous solution using Fe5-AWS adsorbent ( $T = 25^{\circ}\text{C}$ ,  $\text{pH} = 2$ , dosage =  $0.6 \text{ g}/100 \text{ mL}$  and  $C_0 = 10 \text{ mg}\cdot\text{L}^{-1}$ )



$$\frac{t}{q_t} = \frac{1}{K_2 q_e^2} + \frac{t}{q_e} \quad (6)$$

where  $K_2$  ( $\text{g}\cdot\text{mg} \text{ min}^{-1}$ ) is the pseudo-second-order rate constant. From plotting  $t/q_t$  versus  $t$  (Figure 11), the values of  $q_e$  and  $K_2$  can be obtained from the slope and intercept, respectively. Parameters of kinetic models together are presented in Table III.

Table III shows the values of the correlation coefficient for pseudo-first-order adsorption model; they are higher than the value for the pseudo-second-order adsorption. Moreover, the values of adsorption capacities  $q_e$  calculated using the model are

**Figure 11** Pseudo-second-order kinetic plot for the adsorption of Cr(VI) removal from aqueous solution using Fe5-AWS adsorbent ( $T = 25^{\circ}\text{C}$ ,  $\text{pH} = 2$ , dosage =  $0.6 \text{ g}/100 \text{ mL}$  and  $C_0 = 10 \text{ mg}\cdot\text{L}^{-1}$ )

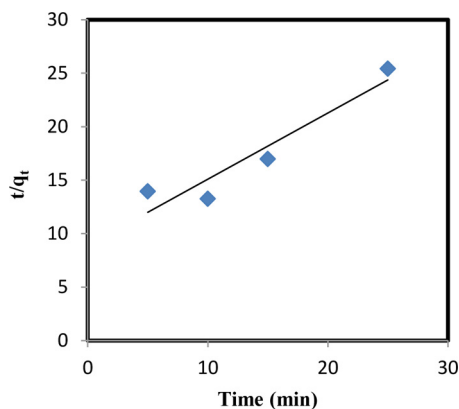


**Table III** Pseudo-first-order and pseudo-second-order kinetics parameters of Cr(VI) adsorption on Fe5-AWS

Sample	Pseudo-first-order			Pseudo-second-order		
	$k_1$ ( $1\cdot\text{min}^{-1}$ )	$q_e$ calc ( $\text{mg}\cdot\text{g}^{-1}$ )	$R^2$	$k_2$ ( $\text{g mg min}^{-1}$ )	$q_e$ calc ( $\text{mg}\cdot\text{g}^{-1}$ )	$R^2$
Fe5-AWS	0.114	1.045	0.978	0.043	1.615	0.896

also close to those determined by experiments. This indicated that the pseudo-first-order adsorption model is more suitable for describing the adsorption kinetics of Cr(VI) on Fe5-AWS.

## 6. Conclusions

This work shows that walnut shell can be used as precursor to produce activated carbon by pyrolysis and physical activation with water vapor. The optimum pyrolysis temperature is  $900^{\circ}\text{C}$  for 2 h at a heating rate of  $10^{\circ}\text{C}\cdot\text{min}^{-1}$  under  $\text{N}_2$  flow. Walnut shell-activated carbon was then used as a supporting material for Fe oxides. Results showed that the walnut shell-activated carbon-supported Fe catalysts (Fe-AWS) obtained at optimal conditions is an effective adsorbent for the removal of Cr(VI) from wastewater than the activated walnut shell obtained without treatment (AWS). Fe5-AWS kinetics for Cr(VI) ions under conditions of  $C_0 = 100 \text{ mg}\cdot\text{L}^{-1}$ , solution volume =  $100 \text{ mL}$ , adsorbent dose =  $1 \text{ g}$ ,  $\text{pH} = 2$  was reached after 60 min and the adsorption capacity was  $10.11 \text{ mg}\cdot\text{g}^{-1}$ ; on the other hand, for AWS 900, the time necessary to attain adsorption equilibrium was longer, 840 min, and the adsorption capacity was  $9.23 \text{ mg}\cdot\text{g}^{-1}$ . The experimental data of the adsorption isotherm follow the Langmuir model and data of the adsorption kinetics follow the pseudo-first-order adsorption model.

## References

- Agarwal, G.S., Hitendra, K.B. and Sanjeev, C. (2006), "Biosorption of aqueous chromium (VI) by Tamarindus indica seeds", *Bioresource Technology*, Vol. 97 No. 7, pp. 949-956.
- Ahmad, B.A., Ala'a, H.A., Gavin, M.W., Stephen, J.A. and Mohammad, N.M.A. (2011), "Retention of toxic chromium from aqueous phase by  $\text{H}_3\text{PO}_4$ -activated lignin: effect of salts and desorption studies", *Desalination*, Vol. 274 Nos 1/3, pp. 64-73.
- Al-Othman, Z.A., Ali, R. and Naushad, M. (2012), "Hexavalent chromium removal from aqueous medium by activated carbon prepared from peanut shell: adsorption kinetics, equilibrium and thermodynamic studies", *Chemical Engineering Journal*, Vol. 184, pp. 238-247.
- Asma, A., Monia, G. and Abdelmottaleb, O. (2015), "Copper supported on porous activated carbon obtained by wetness impregnation: effect of preparation conditions on the ozonation catalyst's characteristics", *Comptes Rendus Chimie*, Vol. 18 No. 1, pp. 100-109.
- Asmaa, F.A. and Muthanna, J.A. (2016), "Mesoporous activated carbon from date stones (*Phoenix dactylifera* L.) by one-step microwave assisted  $\text{K}_2\text{CO}_3$  pyrolysis", *Journal of Water Process Engineering*, Vol. 9, pp. 201-207.
- Cavaco, S.A., Fernandes, S.C., Augusto, M., Quina, M.J. and Gando-Ferreira, L.M. (2009), "Evaluation of chelating ion-exchange resins for separating Cr (III) from industrial effluents", *Journal of Hazardous Materials*, Vol. 169 Nos 1/3, pp. 516-523.
- Chafia, B., Mohamed-Salah, M., Zoubida, M., Fatiha, A., Nassima, R. and Jean-Pierre, B. (2012), "Effects of pyrolysis conditions on the porous structure development of date pits

- activated carbon”, *Journal of Analytical and Applied Pyrolysis*, Vol. 94, pp. 215-222.
- Chand, R., Narimura, K., Kawakita, H., Ohto, K., Watari, T. and Inoue, K. (2009), “Grape waste as a biosorbent for removing Cr(VI) from aqueous solution”, *Journal of Hazardous Materials*, Vol. 163 No. 1, p. 245.
- Daulton, T.L., Little, B.J., Jones-Meehan, J., Blom, D.A. and Allard, L.F. (2007), “Microbial reduction of chromium from the hexavalent to divalent state”, *Geochimica et Cosmochimica Acta*, Vol. 71 No. 3, pp. 556-565.
- Dubey, S.P. and Gopal, K. (2007), “Adsorption of chromium (VI) on low cost adsorbents derived from agricultural waste material: a comparative study”, *Journal of Hazardous Materials*, Vol. 145 No. 3, pp. 465-470.
- Erhan, D., Mehmet, K., Elif, S. and Tuncay, O. (2004), “Adsorption kinetics for the removal of chromium (VI) from aqueous solutions on the activated carbons prepared from agricultural wastes”, *Water SA*, Vol. 30, pp. 533-539.
- Ghadir, N., Hossein, A. and Mohamad, E. (2015), “Batch adsorption of cephalixin antibiotic from aqueous solution by walnut shell-based activated carbon”, *Journal of the Taiwan Institute of Chemical Engineers*, pp. 1-9.
- Hero, M., Ruiz, B., Andrade, M., Mester, A.S., Parra, J.B., Carvalho, A.P. and Ania, C.O. (2012), “Dual role of copper on the reactivity of activated carbons from coal and lignocellulosic precursors”, *Microporous and Mesoporous Materials*, Vol. 154, pp. 68-73.
- Irfan, S., Rohana, A., Wan, S.W.N. and Norita, M. (2015), “Iron impregnated carbon materials with improved physicochemical characteristics”, *Materials Science and Engineering B*, Vol. 201, pp. 1-12.
- Jia-Shun, C., Jun-Xiong, L., Fang, F., Ming-Ting, Z. and Zhi-Rong, H. (2014), “A new adsorbent by modifying walnut shell for the removal of anionic dye: kinetic and thermodynamic studies”, *Bioresource Technology*, Vol. 163, pp. 199-205.
- Jian-hong, X., Nai-yun, G., Dong-ye, Z., Wei-xian, Z., Qin-kun, X. and Ai-hong, X. (2015), “Efficient reduction of bromate in water by nano-iron hydroxide impregnated granular activated carbon (Fe-GAC)”, *Chemical Engineering Journal*, Vol. 275, pp. 189-197.
- Jianping, L., Qingyu, L., Xuehong, Z. and Yan, Y. (2009), “Kinetic parameters and mechanisms of the batch biosorption of Cr(VI) and Cr(III) onto *Leersia hexandra* Swartz biomass”, *Journal of Colloid and Interface Science*, Vol. 333 No. 1, pp. 71-77.
- Juan, Y. and Keqiang, Q. (2010), “Preparation of activated carbons from walnut shells via vacuum chemical activation and their application for methylene blue removal”, *Chemical Engineering Journal*, Vol. 165 No. 1, pp. 209-217.
- Liu, W., Zhang, J., Zhang, C., Wang, Y. and Li, Y. (2010), “Adsorptive removal of Cr (VI) by Fe-modified activated carbon prepared from *Trapa natans* husk”, *Chemical Engineering Journal*, Vol. 162 No. 2, pp. 677-684.
- Maryam, K., Mehdi, A., Shabnam, T., Majdeh, M. and Hamed, R.K. (2008), “Removal of lead, cadmium, zinc, and copper from industrial wastewater by carbon developed from walnut, hazelnut, almond, pistachio shell, and apricot stone”, *Journal of Hazardous Materials*, Vol. 150 No. 2, pp. 322-327.
- Melita, L. and Popescu, M. (2008), “Removal of Cr (VI) from industrial water effluents and surface waters using activated composite membranes”, *Journal of Membrane Science*, Vol. 312 Nos 1/2, pp. 157-162.
- Mohammed, D., Rokiah, H., Mohamad Ibrahim, M.N., Mohd, R. and Othman, S. (2012), “Surface characterization and comparative adsorption properties of Cr(VI) on pyrolysed adsorbents of *Acacia mangium* wood and *Phoenix dactylifera* L. stone carbon”, *Journal of Analytical and Applied Pyrolysis*, Vol. 97, pp. 19-28.
- Muhammad, K.D., Muhammad, R.R.K. and Linda, B.L.L. (2014), “Water remediation using low cost adsorbent walnut shell for removal of malachite green: equilibrium, kinetics, thermodynamic and regeneration studies”, *Journal of Environmental Chemical Engineering*, Vol. 2 No. 3, pp. 1434-1444.
- Nabil, B., Pierre, M., Ali, M., Fayçal, D., Rachida, Z. and Marek, R. (2015), “Suitable organoclays for removing slightly soluble organics from aqueous solutions”, *Journal of Chemical and Pharmaceutical Research*, Vol. 7, pp. 295-306.
- Olmez, T. (2009), “The optimization of Cr(VI) reduction and removal by electrocoagulation using response surface methodology”, *Journal of Hazardous Materials*, Vol. 162 Nos 2/3, pp. 1371-1378.
- Orhan, Y. and Buyukgungor, H. (1993), “The removal of heavy metals by using agricultural wastes”, *Water Science and Technology*, Vol. 28, p. 247.
- Parinda, S. and Paitip, Th. (2012), “Cr(VI) adsorption from electroplating plating wastewater by chemically modified coir pith”, *Journal of Environmental Management*, Vol. 102, pp. 1-8.
- Park, D., Lim, S.R., Yun, Y.S. and Park, J.M. (2007), “Reliable evidences that the removal mechanism of hexavalent chromium by natural biomaterials is adsorption-coupled reduction”, *Chemosphere*, Vol. 70 No. 2, pp. 298-305.
- Pehlivan, E., Tran, H.T., Ouédraogo, W.K.I., Schmidt, C., Zachmann, D. and Bahadir, M. (2013), “Sugarcane bagasse treated with hydrous ferric oxide as a potential adsorbent for the removal of as(V) from aqueous solutions”, *Food Chemistry*, Vol. 138 No. 1, pp. 133-138.
- Phuengprasop, T., Sittiwong, J. and Unob, F. (2011), “Removal of heavy metal ions by iron oxide coated sewage sludge”, *Journal of Hazardous Materials*, Vol. 186 No. 1, pp. 502-507.
- Samson, O.O. and Adedibu, C.T. (2016), “Removal of hexavalent chromium from aqueous solutions by adsorption on modified groundnut hull”, *Journal of Basic and Applied Sciences*, Vol. 5, pp. 377-388.
- Su-Hwa, J., Seung-Jin, O., Gyung-Goo, C. and Joo-Sik, K. (2014), “Production and characterization of microporous activated carbons and metallurgical bio-coke from waste shell biomass”, *Journal of Analytical and Applied Pyrolysis*, Vol. 109, pp. 123-131.
- Sumathi, K.M.S., Mahimairaja, S. and Naidu, R. (2005), “Use of low-cost biological wastes and vermiculite for removal of chromium from tannery effluent”, *Bioresource Technology*, Vol. 96 No. 3, pp. 309-316.

- Thomson, R.C. and Miller, M.K. (1998), "Carbide precipitation in martensite during the early stages of tempering Cr- and Mo-containing low alloy steels", *Acta Materialia*, Vol. 46 No. 6, pp. 2203-2213.
- Uysal, M. and Ar, I. (2007), "Removal of Cr(VI) from industrial wastewaters by adsorption part I: determination of optimum conditions", *Journal of Hazardous Materials*, Vol. 149 No. 2, pp. 482-491.
- Wang, X.J., Wang, Y., Wang, X., Liu, M., Xia, S.Q., Yin, D. Q., Zhang, Y.L. and Zhao, J.F. (2011), "Microwave-assisted preparation of bamboo charcoal-based iron-containing adsorbents for Cr(VI) removal", *Chemical Engineering Journal*, Vol. 174 No. 1, pp. 326-332.
- Wei, W., Xuejiang, W., Xin, W., Lianzhen, Y., Zhen, W., Siqing, X. and Jianfu, Z. (2013), "Cr (VI) removal from aqueous solution with bamboo charcoal chemically modified by iron and cobalt with the assistance of microwave", *Journal of Environmental Sciences*, Vol. 25 No. 9, pp. 1726-1735.
- Xiang, H., Hua, Z. and Zhirong, S. (2017), "Adsorption of low concentration ceftazidime from aqueous solutions using impregnated activated carbon promoted by Iron,

- Copper and Aluminum", *Applied Surface Science*, Vol. 392, pp. 332-341.
- Yahia, A.A. and Hisham, S.B. (2009), "Sulfur removal from model diesel fuel using granular activated carbon from dates' stones activated by ZnCl<sub>2</sub>", *Fuel*, Vol. 88 No. 1, pp. 87-94.
- Yuanyuan, S., Qinyan, Y., Yanpeng, M., Baoyu, G., Yuan, G. and Lihui, H. (2014), "Enhanced adsorption of chromium onto activated carbon by microwave-assisted H<sub>3</sub>PO<sub>4</sub> mixed with Fe/Al/Mn activation", *Journal of Hazardous Materials*, Vol. 265, pp. 191-200.

### Further reading

- Jian-hong, X., Nai-yun, G., Yang, D. and Si-qing, X. (2013), "Nanoscale iron hydroxide-doped granular activated carbon (Fe-GAC) as a sorbent for perchlorate in water", *Chemical Engineering Journal*, Vol. 222, pp. 520-526.

### Corresponding author

**Karima Derdour** can be contacted at: [derdourkarima3@yahoo.com](mailto:derdourkarima3@yahoo.com)